

Predicting Second Gas-Solid Virial Coefficients  
Using Calculated Properties of Molecules

by  
Dana Hooper

Departmental Honors Thesis  
The University of Tennessee at Chattanooga  
Department of Chemistry

Project Director: Tom Rybolt  
Examination Date: March 27, 2002

Committee Members:

Tom Rybolt  
Robert Mebane  
Doug Kutz  
Robert Marlowe  
Gregory O'Dea

Examining Committee Signatures:

Tom Rybolt

Robert Mebane

Doug Kutz

Robert Marlowe

Gregory O'Dea

John Phillippe

Chairperson, University Departmental Honors Committee

## Table of Contents

Abstract	2
Background	3
Theory	8
Previous Work	11
Experimental	13
Analysis and Results	15
Discussion	18
Conclusion	21
References	22
Tables	
Table 1	23
Table 2	25
Table 3	26
Table 4	28
Table 5	29
Table 6	29
Figures	
Carbopack C data: Figure 1-5	30
MR: Figure 6	35
All Data: Figure 7-12	36
Table of Symbols	42

## Abstract

An interesting branch of physical chemistry is the study of the interaction of a molecule (adsorbate) with a surface. This type of interaction occurs in gas chromatography. Retention time is the time it takes for a sample gas to reach a detector at the end of a powder packed gas chromatography column. The second-gas virial coefficient,  $B_{2s}$ , can be related to retention time and to the amount of gas absorbed. For this research, second-gas virial coefficient data was obtained from previously published papers for thirty-five adsorbates at 403 Kelvin. For those adsorbates that did not have data at 403K, values were extrapolated so that all the  $B_{2s}$  values were at the same temperature.  $B_{2s}$  values were measured from adsorption on three different carbon surfaces. The surfaces were Carbopack C, Carbopack B, and Super Sorb, having surface areas of 10, 100, and 3169m<sup>2</sup>/g, respectively.

CAChe, Computer Aided Chemistry software, was used to model the adsorbates and to calculate physical properties, which could then be used to predict the  $\ln B_{2s}$  values. The molecular properties calculated by CAChe were molar refractivity (size of the electron cloud), connectivity index (linearity or branching), and dipole moment (separation of charge in a molecule). Correlations were performed first using the individual carbon surfaces to predict  $\ln B_{2s}$  using each calculated property alone and in combination. Results showed that a combination of molar refractivity, connectivity index and dipole moment was a better predictor of  $\ln B_{2s}$  than any of those properties alone.

When plotting all of the data together, the surface area was brought in as a correlation property to allow for all the data to be combined. An overall correlation of  $r^2 = 0.9566$  was found when  $\ln B_{2s}$  was predicted by molar refractivity, connectivity index, dipole moment, and surface area.

This research has possible application in the material adsorption of harmful molecules, such as those used in chemical warfare. It also has important scientific application in that it makes it possible to accurately predict gas chromatographic retention times and the amount of gas adsorbed on a solid surface using easily calculated physical properties of a molecule without having to go into the lab and determine the values experimentally.

## **Background**

The Quantitative Structure-Property Relationship (QSPR) describes the relationship between molecular calculated properties based on molecular structure and experimental physical properties. Computers have revolutionized the ability of chemists to calculate, compute, and analyze data. Chemists are now able to do complex calculations in minutes or seconds that would otherwise have to be done by hand. Through QSPR we can use computers to calculate properties that make it possible to replace laboratory experiments to determine certain properties of molecules.

The Quantitative Structure-Retention Relationship (QSRR) refers to the connection between the structures of gas adsorbate molecules and their

chromatographic retention times or related data (1). For the work described here, a QSRR was determined using properties calculated by CAChe, Computer Aided Chemistry Software, and used to predict the  $B_{2s}$  value of a series of adsorbates. The second gas-solid virial coefficient,  $B_{2s}$  is related to the moles of gas adsorbed per gram of adsorbent in a gas chromatographic column.  $B_{2s}$  represents the interaction of isolated adsorbate molecules with a solid surface.  $B_{2s}$  values vary with temperature and contain information about the structure of the solid as well as the strength and nature of gas-solid interactions (5). The more strongly an adsorbate is attracted to an adsorbent the larger the corresponding  $B_{2s}$  value. For this research we are interested in the physical adsorption of adsorbates onto a surface due to van der Waals interactions. Van der Waals interactions have a long range but are weak (6). This is different from chemical adsorption where actual chemical bonds are formed between atoms.

The gas phase molecules that are attracted to the surface are called the adsorbates, and the surface to which the adsorbate is attracted is called the adsorbent. The interaction between the adsorbate and adsorbent may be described in terms of a potential energy well, where there is an optimum distance between the adsorbate and surface atoms. A decrease in the optimum distance would result in repulsive forces. The extent to which the adsorbate is attracted to the surface is dependant on temperature and the surface area of the adsorbent. The experimental determination of  $B_{2s}$  requires experimental measurements of corrected retention time, flow rate in the gas chromatographic column, adsorbent temperature, room temperature, column inlet

pressure and column outlet pressure. Specifics of calculating  $B_{2s}$  values and experimental methods used in this research may be found in the Theory and Experimental sections of this paper, respectively.

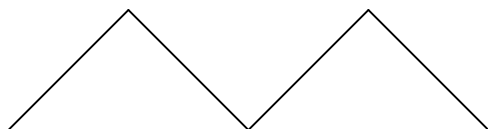
The gas chromatographic columns were commercially packed with carbon powders having various surface areas. The carbons surfaces used in this work are Carbpac C, Carbpac B, and Super Sorb, having measured BET surface areas of 10, 100, and 3169 m<sup>2</sup>/g, respectively. Carbpac C and Carbpac B are nonporous nonspecific, highly inert graphite carbon adsorbents which separate compounds according to the size and shape of the molecule and its polarizability (7). Super Sorb is an example of activated carbon. The microcrystalline structure of the carbon is similar to graphite where the crystals consist of parallel layers of hexagonal rings which are bound by covalent bonds to three adjoining carbons with a fourth group of delocalized  $\pi$  electrons that may move freely in the structure (8). Activated carbon structures differ from graphite structures in that the interlayer distance are unequal in the active carbon and that activated carbon tends to have a lower order of structure (9). Activated carbons are mainly used as adsorbents, catalyst supports and electrode materials. Their specific use is determined by their crystalline makeup, which depends on the raw material and the method of preparing the carbon. The production method affects the pore shape and size of the carbon, designated as macropores, mesopores, and micropores, which correspond to large, medium, and small pore size. Mesopores and micropores are used in adsorption measurements. Heteroatoms may be eliminated by burn-off at temperatures over 1000°C (9).

Previous research has shown that it is possible to predict  $B_{2s}$  values using calculated physical properties of the adsorbates (1-4). The properties used in this research are molar refractivity, connectivity index, and dipole moment. Each of these properties were calculated using CAChe.

Molar refractivity, MR relates to the overall size of the electron cloud, or the polarizability of the molecule.  $MR = (4\pi N\alpha/3)$  where N is Avogadro's number and  $\alpha$  is the polarizability. For this research molar refractivity was calculated using CAChe's atom typing scheme. It may also be calculated using published tables of values for fragments of molecules. The molecule is broken into a few fragments and the molar refractivity for those individual fragments are added together to obtain the total molar refractivity for the molecule. Tables of molar refractivity values may be found in the literature (10). For some molecules used in previous work, molar refractivity was calculated by hand and using CAChe. It was found that the two values agree (1).

Connectivity index,  $\chi$ , relates to the linearity or branching of a molecule. It increases as the molecule becomes larger and more extended (less branched). The connectivity index can also be calculated by hand using the equation  $\chi = \sum(\delta_i\delta_j)_s^{-1/2}$ , where  $\delta$  stands for the number of adjacent bonded nonhydrogen atoms and s represents each bond in a molecule (1). This is best demonstrated by example. Pentane will be used as the example here.

In the pentane structure each atom is given a number that corresponds to the number of adjacent atoms. Then above formula is then used to calculate the connectivity index for pentane.



These numbers are then added together to give the connectivity index for the molecule. This method is independent of the types of atoms in the molecule. For pentane, the  $\chi = 2.414$ . Previous work has shown that the values, when calculated by this method, correlate closely to the CAChe calculated values (1).

The dipole moment,  $\mu$ , consists of two electric charges separated by a distance (6). Magnitudes of dipole moments are reported in debye, D. The dipole moments were calculated using CAChe's DFT (density functional theory) B88-PW91. CAChe has the ability to calculate dipole moment using a variety of methods. In order to determine which of these should be used for this research, they were correlated with experimentally determined dipole moments from Lange's Handbook of Chemistry. These correlations were performed by another of Dr. Rybolt's research students, Jason Harwood. The method determined to correlate best with the experimental method was the B88-PW91 method. Additional information about the technique CAChe uses to calculate dipole moment may be found in the Theory

section of this paper. It was correlated with the experimental dipole moment with an  $r^2$  value of 0.9864 and an average deviation of 0.107 for 35 molecules.

## Theory

In the Henry's Law region of low coverage adsorption, the retention time of an adsorbate gas is directly proportional to the  $B_{2s}$  value (1).

$B_{2s}$  may be calculated with the equation

$$B_{2s} = (t F_1/m) \quad (1)$$

Where  $t$  is the retention time,  $F_1$  is the corrected flow rate of the gas chromatographic column, which is dependent on the inlet pressure, outlet pressure, atmospheric pressure, and the temperature of the flow meter, and  $m$  is the mass of the solid adsorbent. The retention time in the above equation is actually the corrected retention time and is found by the following equation:

$$t = t_s - t_m \quad (2)$$

where  $t_m$  is the time from injection to detection of pulse maximum of a suitable marker gas with negligible solid-gas interaction and  $t_s$  is the time from injection to detection of pulse maximum of the sample gas.

For a uniform, flat surface  $B_{2s}$  may be expressed as

$$B_{2s} = Az^* \int [\exp(u_{1s}(y)/kT) - 1] dy \quad (3)$$

where  $A$  is the surface area of the adsorbent,  $z^*$  is the equilibrium internuclear gas-solid separation,  $u_{1s}$  is the gas-solid interaction potential,  $y$  is a reduced variable distance where  $y=z/z^*$ ,  $k$  is the Boltzmann constant, and  $T$  is the temperature (5).

In order to simplify the math, an approximation of the above equation was derived by Hansen (1):

$$B_{2s} = Az^* (2\pi/nm)^{1/2} (T/E^*)^{1/2} \exp(E^*/T). \quad (4)$$

It has been shown in previous work that the molar refractivity may be correlated with  $E^*$ , the interaction energy or depth of the gas-solid potential well at equilibrium separation, in the following equation (1):

$$E^* = B(MR) + i \quad (5)$$

where  $MR$  is the molar refractivity,  $B$  is the slope of the correlation, and  $i$  is the intercept.

By substituting this equation into the approximated equation above and taking the natural logarithm of both sides, the resulting equation is

$$\ln B_{2s} = \ln [Az^*((2\pi/nm)^{1/2})] - 0.5 \ln[B(MR)/T + i/T] + i/T + (B/T)(MR). \quad (6)$$

Previous research correlated  $E^*$  with the molar refractivity and the connectivity index,  $\chi$ , with  $\ln z^*$  (1). This resulted in the equation

$$\ln B_{2s} = a(MR) + b(\chi) + c \quad (7)$$

where  $a$ ,  $b$ , and  $c$  are empirical constants.

In the current work, a different approach was used. Rearranging equation 4 and taking the natural logarithm gives

$$\ln B_{2s} = \ln (2\pi T/nm)^{1/2} + \ln A + E^*/T + \ln (z^*/E^{*1/2}). \quad (8)$$

At a fixed temperature  $\ln(2\pi T/nm)^{1/2}$  may be considered to be a constant. We then assume  $E^*/T$  may be correlated with molar refractivity, connectivity index, and dipole moment using the following equation:

$$E^*/T = a(MR) + b(\chi) + d(\mu) + c \quad (9)$$

where a, b, c, d are constants. It is known that the parameters above are proportional to the strength of molecule-molecule and molecule-surface interactions.

Using this correlation, we were able to deduce the equation

$$\ln B_{2s} = \ln A + a(MR) + b(\chi) + d(\mu) + g \ln (z^*/E^{*1/2}) + c. \quad (10)$$

The  $\ln (z^*/E^{*1/2})$  was found to be proportional to  $\ln (V_m^{1/3}/MR^{1/2})$  because  $E^*$  is proportional to  $MR$  and for an assumed spherical shape,  $V_m$ , molar volume, is proportional to  $z^{*3}$  from  $V=4/3\pi r^3$ . When  $\ln (V_m^{1/3}/MR^{1/2})$  is substituted into the above equation we obtain:

$$\ln B_{2s} = \ln A + a(MR) + b(\chi) + d(\mu) + g \ln (V_m^{1/3}/MR^{1/2}) + c. \quad (11)$$

A more simplistic approach to this equation is

$$\ln B_{2s} = \ln A + a(MR) + b(\chi) + d(\mu) + c \quad (12)$$

where only  $MR$ ,  $\chi$ , and  $\mu$  are used to predict  $\ln B_{2s}$  values. Each of these equations is explored in more detail in the Analysis and Results section of this paper.

In this research we use the dipole moment as a predictor of  $\ln B_{2s}$  values. The method used to calculate the dipole moment is the B88-PW91 method from CAChe. It utilizes density functional theory to calculate the dipole moment. Density functional theory (DFT) uses the concept of electron probability density and electron correlation which involves less demanding computation than alternative methods.

DFT expresses the energy of an electronic system in terms of the electron probability density, which is a function of electron density (11).

### **Previous Work**

The initial portion of this project began in Fall 1999. This work is based on previous research by Dr. Rybolt and former students.  $B_{2s}$  data were collected by Dr. Howard Thomas and a student during the summer of 1999 and then given to Dr. Rybolt for analysis. The samples consisted of ten sulfur-containing compounds including ethanethiol, 1-propanethiol, methyl sulfide, 2-propane thiol, 1-methyl-1-propanethiol, 2-methyl-1-propanethiol, 2-methyl-2-propanethiol, methyl sulfide, ethyl methyl sulfide, and tert-butyl methyl sulfide. The column used for gas chromatography was packed with Carbopack C, a carbon powder with a having a surface area of  $10\text{m}^2/\text{g}$ . The measurements were taken over a range of temperatures and then extrapolated, if needed, to 403K for analysis.

We began the analysis by drawing the compounds with CAChe Software, version 4.1 (Fujitsu Inc.) running on a Power Macintosh 7100 or Macintosh G3 computer. CAChe was then used to calculate physical properties of the compounds (molar refractivity and connectivity index) and to create regression plots to predict  $B_{2s}$  values using the calculated properties of MR and  $\chi$ .

Using the theoretical equation as a starting point (Equation 4) it is possible to correlate parameters in the equation with physical properties of the compounds. Molar refractivity was determined to be proportional to  $E^*$ , the solid-gas interaction

energy. Connectivity index was determined to be proportional to  $z^*$ , the equilibrium internuclear gas-solid separation. By substituting these properties into the theoretical equation, we were able to obtain an equation that incorporated calculated values in place of those values that have to be experimentally determined. The most easily applied equation is the following:

$$\ln B_{2s} = a(\text{MR}) + b(\chi) + c \quad (13)$$

where a, b, and c are coefficients. Applying this equation to the sulfur  $\ln B_{2s}$  data, having ten data points, an  $r^2$  value of 0.989 was obtained. The  $r^2$  value was higher when using both MR and  $\chi$  in combination versus either of these alone. For example, when predicting the  $\ln B_{2s}$  using MR as the only parameter, the  $r^2$  value is 0.961. By adding the  $\chi$  as a parameter, the  $r^2$  value is increased to the above value (1).

In addition to the sulfur-containing compounds, we attempted to correlate the published retention times of 373 organic molecules with their physical properties. (11) First, these molecules were divided into groups based on their functionality. These groups were alcohols, aldehydes, alkanes, alkenes, benzenes, cycloalkanes, dienes, esters, ethers, and ketones. The molecules were then drawn in the CAChe program and their MR and  $\chi$  were calculated. By applying the same form of equation 13, an  $r^2$  value of 0.982 was obtained for these molecules. The results of this study demonstrate how just two calculated properties may be used to correlate retention times for a large number of diverse molecules.

This work shows how the properties of molar refractivity and connectivity index may be used to predict the  $B_{2s}$  values of various adsorbates. By using a

computer program capable of calculating physical properties in a timely manner, one is able to avoid going into the lab to experimentally determine the retention times of these molecules, provided that a valid correlation is first established for a set of experimental values. By first correlating molar refractivity and connectivity index with parameters in the theoretical equation, we have a basis with which to support our final equation.

## **Experimental**

The experimental portion of this work was performed by Dr. Howard Thomas and students over a period of years. The sulfur-containing compound data were collected during the summer of 1999. This work is part of an on-going collaboration between Dr. Rybolt and Dr. Thomas in the study of physical adsorption on various surfaces.

Gas-solid second virial coefficient values were determined for various gaseous samples using a Perkin-Elmer 3920A gas chromatograph with a thermal conductivity detector. Data were collected over a range of temperatures as close as possible to 403K. When possible, measurements were made at  $403 \pm 0.5$ K. The experimental procedure used for each specific group of samples may be found in their respective papers (1-4). The data was collected using columns packed with Carbo-pack C, Carbo-pack B, and Super Sorb, having BET N<sub>2</sub> adsorption surface areas of 10, 100, and 3169 m<sup>2</sup>/g, respectively. The Carbo-pack C column was packed by Supelco Inc and contained 2.78g of 60/80-mesh Carbo-pack C. The 60/80 mesh

Carbopack B column was also packed by Supelco and contained 2.96g. The Super Sorb sample, having a mass of 0.4785g, was packed into a U-shaped column. It was obtained from Amoco Research and characterized by a Micrometrics Digisorb 2500 automatic surface area and pore volume analyzer. Each column was outgassed at a temperature of 623K for 12 to 14 hours to remove any residual sample from the surface prior to making adsorption measurements. Gas adsorbates were injected using a Hamilton gas syringe with neon as the marker gas for the Carbopack C and Carbopack B. The marker gas is used to determine the time required for a gas to pass through the column with no interactions with the surface. The actual retention time for an adsorbate, or the retention time due to gas-solid interactions, is calculated by subtracting the retention time for the marker gas from the actual retention time for the adsorbate (see Equation 2). A soap bubble flow meter is used to measure the flow rates. Each adsorbate's retention time is measured several times at each temperature, varying the amount of gas injected. By plotting the retention times versus the injection volume, it is possible to extrapolate to zero sample size, and that value is used in the calculation of  $B_{2s}$ .

In order to calculate the  $B_{2s}$  value, it is necessary to know the following information: the column temperature, soap bubble flow time, retention time of adsorbate, retention time of marker gas, the corrected retention time, atmospheric pressure, vapor pressure of water, mass of the adsorbent, room temperature, and the septum pressure. A detailed approach to calculation of  $B_{2s}$  values may be found in the literature (5). It has been previously determined that a plot of  $\ln B_{2s}$  versus  $1/T$ ,

where  $T$  is the temperature, should yield a linear plot for a given system. Given this, it is possible to extrapolate a  $B_{2s}$  value at a particular temperature for a specified adsorbate.

## **Analysis and Results**

The recent portion of this project began by selecting compounds and data. This data were selected from four previously published papers containing  $B_{2s}$  data (1-4). The four papers contained data on three different surfaces, Carbopack C, Carbopack B, and Super Sorb. having surface areas of 10, 100 and 3169  $m^2/g$ , respectively. The selected samples and their corresponding  $B_{2s}$  values and surface areas may be seen in Table 1.

Since  $B_{2s}$  measurements are temperature dependent, it was necessary to have values at the same temperature for all data. The data for Carbopack B and Super Sorb were not given at the desired 403K, making it necessary to extrapolate. Extrapolation was achieved by plotting  $\ln B_{2s}$  versus  $1/T$  where  $T$  is the temperature in Kelvin. Previous work has shown that  $\ln B_{2s}$  vs.  $1/T$  gives a good correlation of data over a temperature range (5). The plotting of  $\ln B_{2s}$  vs.  $1/T$  is standard practice in virial adsorption analysis. This plot should be linear (see Equation 8) with a slope of  $E^*$ . The plots cover the range of temperatures over which the measurements were taken. A list of the extrapolation equations and resulting temperatures at 403K may be seen in Table 2. The five samples that were extrapolated outside their range of measured temperatures are marked on the table.

The samples were then drawn using the computer program CAChe, Computer Aided Chemistry software, Version 5.0 (Fujitsu Inc.) running on a PC. Once the samples were drawn, CAChe was used to calculate all the physical properties used to correlate with  $B_{2s}$  values. The properties used were molar refractivity, connectivity index, and dipole moment, which are discussed elsewhere in this paper. Table 3 shows the values of MR,  $\chi$ , and  $\mu$  calculated using CAChe.

First, the correlations were performed using individual carbon surfaces, Carbpacck C, Carbpacck B, and Super Sorb. Correlation plots were obtained using each of the properties alone and in combination. Table 4 shows the results of each correlation and the respective  $r^2$  values. Figures 1-5 shows the plots for Carbpacck C. Observation of the  $r^2$  values show that a combination of properties resulted in a higher  $r^2$  value than any of the other properties alone. Figure 1 uses MR to predict  $\ln B_{2s}$  with an  $r^2$  value of 0.9182. Figure 2 uses  $\chi$  to predict  $\ln B_{2s}$  with an  $r^2$  value of 0.6612. Figure 3 uses  $\mu$  to predict  $\ln B_{2s}$  with an  $r^2$  value of 0.0007. By combining the calculated properties, we are able to obtain higher  $r^2$  values. Figure 4 uses MR and  $\chi$  to predict  $\ln B_{2s}$  with an  $r^2$  value of 0.9196. Figure 5, where all three calculated properties, MR,  $\chi$ , and  $\mu$  are used to predict  $\ln B_{2s}$  gives an  $r^2$  value of 0.9198. These figures demonstrate how a combination of properties are more useful in predicting  $\ln B_{2s}$  than any single property alone for an individual carbon surface. These results were similar to those obtained for the Carbpacck B and SuperSorb plots in that the  $r^2$  value increased as more properties were added to the correlation equation. For example, using MR,  $\chi$ , and  $\mu$  in combination resulted in a better correlation with  $\ln$

$B_{2s}$  than either of these properties used alone. Table 4 shows the results for each of the three surfaces, Carbopack C, Carbopack B, and Super Sorb. For each of the surfaces, the combination of MR,  $\chi$ , and  $\mu$  gave the highest  $r^2$  value, and thus the best prediction of  $\ln B_{2s}$ .

In order to successfully plot the data with all three surfaces on one plot, it is necessary to have a property that will allow for the data to be combined. This problem became evident when all the data were plotted using molar refractivity as the correlation property. Figure 6 shows three distinct lines in the plot, each corresponding to a different surface area. The uppermost line corresponds to Super Sorb, the middle to Carbopack B, and the lower line to Carbopack C. To solve this problem of separation of surfaces we were able to bring the surface area into the correlation. The natural logarithm of the surface area was used and is consistent with the theory as shown in Equation 6 where the  $\ln$  surface area is proportional to  $\ln B_{2s}$ . In order to determine if this method would be useful, we plotted  $\ln B_{2s}$  versus  $\ln$  surface area for four different gases for which we have data on all three surfaces. These adsorbates were propane, dichloromethane, chloromethane, and chlorodifluoromethane. As seen in Table 5 all four of these samples demonstrated high  $r^2$  values, indicating that the  $\ln$  surface area will be a useful property to use in the correlations.

By correlating the surface area, molar refractivity, connectivity index, and dipole moment with  $\ln B_{2s}$ , plots were prepared using each property alone and then in

combination. Table 6 summarizes the correlation coefficients for these plots shown in Figures 7-12.

Figure 7 is derived from Equation 11. The  $\ln (V_m^{1/3} / MR^{1/2})$  is included in the prediction on  $\ln B_{2s}$ . When this “size factor” is included in the correlation, an  $r^2$  value of 0.9623 is obtained.

Each of the Figures (8-12) use the  $\ln$  surface area as a correlation property to allow all the data to be combined. In Figure 8 MR is used to predict  $\ln B_{2s}$  with an  $r^2$  value of 0.9534.  $\chi$  and  $\mu$  (Figures 9 and 10) used alone give  $r^2$  values of 0.7759 and 0.4307, respectively. When MR and  $\chi$  are used together an  $r^2$  value of 0.9562 is obtained as shown in Figure 11. By combining all three of the calculated properties, MR,  $\chi$ ,  $\mu$ , an  $r^2$  value of 0.9566 is obtained as shown in Figure 12. Here, as when plotting single surface data, the combination of calculated properties yields a higher  $r^2$  value and are thus better predictors of  $\ln B_{2s}$  than either property alone.

## Discussion

Using the data from CarboPack C as an example, it is possible to see the predictive power of each of the physical properties, molar refractivity, connectivity index, and dipole moment, alone and in combination for a single surface. Using molar refractivity alone, an  $r^2=0.9163$  was obtained. For connectivity alone,  $r^2=0.6613$  and for dipole moment alone  $r^2=0.0007$ . However, when these three properties were used in combination, they predicted the  $\ln B_{2s}$  values with an  $r^2=0.9199$ , a value higher than with any of the properties used alone.

Table 4 shows the results of similar plots using the Carbopack B and Super Sorb individually. For Carbopack B the correlation coefficient for predicting  $\ln B_{2s}$  using all three calculated properties was  $r^2=0.9796$ . Super Sorb demonstrated an even higher  $r^2$  value when all three properties were combined, 0.9855. As seen on Table 4, by combining the molar refractivity, connectivity index, and dipole moment, it was possible to accurately predict  $B_{2s}$  values for the adsorbates on a single surface.

Figure 6 is representative of the result when all of the data were first combined into one plot. Figure 6 is a plot of the  $\ln B_{2s}$  versus molar refractivity. One can clearly see three distinct lines occurring on the plot. These three distinct regions on the graph correspond to the three surfaces on which the  $B_{2s}$  measurements were taken. The top group corresponds to those adsorbates measured on Super Sorb. The middle group corresponds to those adsorbates measured on Carbopack B and the lower group corresponds to those adsorbates measured on Carbopack C. These results are consistent with the observation that Carbopack C, having the smallest surface area, leads to smaller  $B_{2s}$  values, followed in magnitude by Carbopack B and finally Super Sorb. This may be observed in Table 1. In order to correct the problem of observing three distinct lines when all the data are plotted together, the surface area was brought in as a parameter. In order to do this, we determined that the surface area may be correlated to  $\ln B_{2s}$ . Table 5 shows the results of plotting  $\ln B_{2s}$  versus the  $\ln$  surface area for four adsorbates for which there was data available for all three surfaces. As seen on Table 5, the  $r^2$  values were very high, all around  $r^2=0.999$ . The

natural log of the surface area was used in order to be consistent with the theoretical equation (Equation 6).

Table 6 gives a summary of the correlation coefficients obtained with the combined data. Each calculated physical property, molar refractivity, connectivity index, and dipole moment, were used as predictors of  $\ln B_{2s}$  alone and in combination. Figure 7 includes MR,  $\chi$ ,  $\mu$ ,  $\ln$  surface area, and  $\ln (V_m^{1/3}/MR^{1/2})$ , giving an  $r^2$  value of 0.9623. Figure 8 shows a plot using molar refractivity as the predictor of  $\ln B_{2s}$  with an  $r^2$  value of 0.953. Connectivity index alone gives an  $r^2$  value of 0.7759, and dipole moment alone gives an  $r^2$  value of 0.4307. When just the molar refractivity and connectivity index are used to predict  $\ln B_{2s}$ , the  $r^2$  value is 0.9562, as seen in Figure 11. The addition of dipole moment to molar refractivity and connectivity index in predicting  $\ln B_{2s}$  increases the  $r^2$  value to 0.9566. Though this is only a slight improvement, it is consistent with the individual surface results in that the combination of properties gives a better prediction of  $\ln B_{2s}$  than any of those properties alone. Although, the prediction in Figure 7 has a higher  $r^2$  value than Figure 12 (0.9623 versus 0.9562) we prefer the prediction where only molar refractivity, connectivity index, dipole moment, and the  $\ln$  surface area are used in order to keep the equation as simple as possible and still achieve an acceptable  $r^2$  value.

## **Conclusion**

The significance of this work is that it demonstrates how calculated physical properties of the adsorbate molecules may be used to predict experimental  $\ln B_{2s}$  data. It is also notable that a combination of calculated physical properties are a better predictor of  $\ln B_{2s}$  than any single property alone.

Another important aspect of this study is that we were able to combine data from three different surface areas on the same plot by using the  $\ln$  surface area as a parameter to represent adsorbent differences.

Some possible future work for this study would be to collect data on other surfaces and see if it may be combined with this data to give acceptable correlation coefficients.

## References

1. Rybolt, T.R., Hooper, D.N., Stensby, J.B., Thomas, H.E., Baker, M.L., *J. Colloid Interface Sci.* **234**, 168-177 (2001).
2. Rybolt, T.R., Zhang, X., Wall, M.D., Thomas, H.E., Mullinax, L.E., Lee, J.R., *J. Colloid Interface Sci.* **149**, 359-366 (1992).
3. Rybolt, T.R., Logan, D.L., Milburn, M.W., Thomas, H.E., Waters, A.B., *J. Colloid Interface Sci.* **220**, 148-156 (1999).
4. Rybolt, T.R., Epperson, M.T., Weaver, H.W., Thomas, H.E., Clare S.E., Manning, B.M., McClung, J.T., *J. Colloid Interface Sci.* **173**, 202-210 (1995).
5. Tybolt, T.R., Thomas, H.E., "Henry's Law Behavior in Gas-Solid Chromatography: A Virial Approach" *Interfacial Phenomena In Chromatography* ed. Emile Pefferkorn, Marcel-Dekker, p. 1-40, 1999.
6. Rich, Ronald L. *J. Chem. Ed.* **72**, 9-12 (1995).
7. Supelco Inc. Chromatography Products Catalog p. 40, Supelco Park. Belefonte, PA 1999.
8. Atkins, Peter, *Physical Chemistry* 6<sup>th</sup> edition, W.H. Freeman and Company, New York, 1998.
9. Kaneko, K., Ishii, C., Rybolt, T., "Superhigh Surface Area Determination of Microporous Carbons" *Studies in Surface Science and Catalysis* Elsevier Science B.V. p. 538-592, 1994.
10. Hansch, Corwin, and Leo, Albert, *Exploring QSAR* American Chemical Society, Washington, D.C., 1995.
11. Jankowska, Helena, Swiatkowski, Andrezej, Choma, Jerry, *Active Carbon* Ellis Horwood, NY, p. 75-100, 1991.
12. Pompe, M., and Novic, M., *J. Chem. Inf. Comput. Sci.* **39** 59 (1999).

Table 1  
 $B_{2s}$  values and corresponding surface area for adsorbates

<b>Molecular Formula</b>	<b>Chemical Sample</b>	<b><math>B_{2s}</math> value</b>	<b><math>\ln B_{2s}</math></b>	<b>Surface Area(m<sup>2</sup>/g)</b>
C <sub>1</sub> Cl <sub>4</sub>	Tetrachloromethane	6.00	1.79	10
C <sub>1</sub> Cl <sub>4</sub>	Tetrachloromethane	141	4.95	100
C <sub>1</sub> F <sub>2</sub> Br <sub>2</sub>	Dibromodifluoromethane	1.69	0.525	10
C <sub>1</sub> F <sub>2</sub> Cl <sub>2</sub>	Dichlorodifluoromethane	0.340	-1.08	10
C <sub>1</sub> F <sub>2</sub> Cl <sub>2</sub>	Dichlorodifluoromethane	500	6.21	3169
C <sub>1</sub> FCI <sub>3</sub>	Trichlorofluoromethane	1.56	0.444	10
C <sub>1</sub> FCI <sub>3</sub>	Trichlorofluoromethane	91.5	4.52	100
C <sub>1</sub> H <sub>2</sub> Cl <sub>2</sub>	Dichloromethane	0.650	-0.431	10
C <sub>1</sub> H <sub>2</sub> Cl <sub>2</sub>	Dichloromethane	12.9	2.56	100
C <sub>1</sub> H <sub>2</sub> Cl <sub>2</sub>	Dichloromethane	1590	7.37	3169
C <sub>1</sub> H <sub>2</sub> ClBr	Bromochloromethane	1.44	0.36	10
C <sub>1</sub> H <sub>3</sub> Cl	Chloromethane	0.110	-2.21	10
C <sub>1</sub> H <sub>3</sub> Cl	Chloromethane	1.69	0.525	100
C <sub>1</sub> H <sub>3</sub> Cl	Chloromethane	160	5.08	3169
C <sub>1</sub> H <sub>3</sub> F	Fluoromethane	31.2	3.44	3169
C <sub>1</sub> HCl <sub>3</sub>	Trichloromethane	2.70	0.993	10
C <sub>1</sub> HCl <sub>3</sub>	Trichloromethane	66.3	4.19	100
C <sub>1</sub> HF <sub>2</sub> Cl	Chlorodifluoromethane	0.130	-2.04	10
C <sub>1</sub> HF <sub>2</sub> Cl	Chlorodifluoromethane	1.93	0.658	100
C <sub>1</sub> HF <sub>2</sub> Cl	Chlorodifluoromethane	208	5.34	3169
C <sub>1</sub> HFCI <sub>2</sub>	Dichlorofluoromethane	6.39	1.85	100
C <sub>2</sub> H <sub>6</sub>	Ethane	1.00	0.00	100
C <sub>2</sub> H <sub>6</sub>	Ethane	49.6	3.90	3169
C <sub>2</sub> H <sub>6</sub> O	Dimethyl Ether	5.63	1.73	100
C <sub>2</sub> H <sub>6</sub> S	Ethanethiol	0.940	-0.062	10
C <sub>2</sub> H <sub>6</sub> S	Dimethyl sulfide	1.05	0.049	10
C <sub>3</sub> H <sub>6</sub> Cl <sub>2</sub>	1,2-dichloropropane	12.2	2.50	10
C <sub>3</sub> H <sub>8</sub>	Propane	0.264	-1.33	10
C <sub>3</sub> H <sub>8</sub>	Propane	4.96	1.60	100
C <sub>3</sub> H <sub>8</sub>	Propane	372	5.92	3169
C <sub>3</sub> H <sub>8</sub> S	1-propanethiol	3.56	1.27	10
C <sub>3</sub> H <sub>8</sub> S	2-propanethiol	2.50	0.916	10

C <sub>3</sub> H <sub>8</sub> S	Ethyl methyl sulfide	3.10	1.13	10
C <sub>4</sub> H <sub>10</sub>	Butane	1.36	0.307	10
C <sub>4</sub> H <sub>10</sub>	Butane	29.4	3.38	100
C <sub>4</sub> H <sub>10</sub>	2-methyl propane	15.4	2.73	100
C <sub>4</sub> H <sub>10</sub> O	Diethyl ether	94.7	4.55	100
C <sub>4</sub> H <sub>10</sub> S	1-methyl-1-propanethiol	8.90	2.19	10
C <sub>4</sub> H <sub>10</sub> S	2-methyl-1-propanethiol	8.30	2.12	10
C <sub>4</sub> H <sub>10</sub> S	2-methyl-2-propanethiol	4.90	1.59	10
C <sub>4</sub> H <sub>10</sub> S	Diethyl sulfide	11.1	2.41	10
C <sub>4</sub> H <sub>9</sub> Cl	1-chlorobutane	11.0	2.40	10
C <sub>5</sub> H <sub>11</sub> Cl	1-chloro-2-methylpropane	8.30	2.12	10
C <sub>5</sub> H <sub>12</sub>	Pentane	6.70	1.90	10
C <sub>5</sub> H <sub>12</sub>	Pentane	163	5.09	100
C <sub>5</sub> H <sub>12</sub> S	tert-Butyl methyl sulfide	28.5	3.35	10
C <sub>6</sub> H <sub>12</sub>	Cyclohexane	7.60	2.03	10
C <sub>6</sub> H <sub>14</sub>	Hexane	45.0	3.81	10
C <sub>6</sub> H <sub>14</sub>	Hexane	931	6.85	100
C <sub>7</sub> H <sub>16</sub>	Heptane	5006	8.52	100
F <sub>6</sub> S	Sulfur hexafluoride	0.950	-0.053	100

Table 2  
 $B_{2s}$  extrapolations to 403K

Super Sorb (3169m <sup>2</sup> /g)		
Adsorbate	Equation	$B_{2s}$ at 403K
Ethane	$y=2836.6x - 3.1341$	49.6
Propane	$y=4113x-4.2861$	372
Chloromethane	$y=3744.8x-4.2192$	160
*Dichloromethane	$y=4964x-4.9462$	1590
Fluoromethane	$y=3265.6x-4.6644$	31.2
Chlorodifluoromethane	$y=4101.5x-4.8415$	208
Dichlorodifluoromethane	$y=4184.5x-4.1687$	500
Carbopack B (100m <sup>2</sup> /g)		
Adsorbate	Equation	$B_{2s}$ at 403K
Ethane	$y=2498.7x-6.1997$	1.0
Chloromethane	$y=3042.5x-7.0276$	1.69
Chlorodifluoromethane	$y=3119.8x-7.082$	1.93
*Sulfur hexafluoride	$y=2551.8x-6.3807$	0.95
Dimethyl ether	$y=3219.2x-6.2606$	5.63
Propane	$y=3616.6x-7.3733$	4.96
Dichlorofluoromethane	$y=3795.3x-7.5627$	6.39
Butane	$y=4599.7x-8.0342$	29.4
2-methyl propane	$y=3648.6x-6.3203$	15.4
*Pentane	$y=5411.4x-8.3351$	163
*Hexane	$y=6327.4x-8.8649$	931
*Heptane	$y=7158.1x-9.2435$	5006
Trichloromethane	$y=4956.2x-8.1036$	66.3
*Tetrachloromethane	$y=4972.8x-7.3884$	141
Trichlorofluoromethane	$y=4849.9x-7.5186$	91.5
Diethyl ether	$y=5244.7x-8.4638$	94.7

\* extrapolated outside range of experimental  $B_{2s}$  values

Table 3  
Calculated Molar Refractivity, Connectivity Index, and Dipole Moment for  
adsorbates

Molecular Formula	Chemical Sample	MR	c	m	Vm (nm <sup>3</sup> )
C <sub>1</sub> Cl <sub>4</sub>	Tetrachloromethane	26.272	2.00	0.009	0.05405
C <sub>1</sub> F <sub>2</sub> Br <sub>2</sub>	Dibromodifluoromethane	22.22	2.00	0.441	0.4777
C <sub>1</sub> F <sub>2</sub> Cl <sub>2</sub>	Dichlorodifluoromethane	16.603	2.00	0.281	0.3966
C <sub>1</sub> FCI <sub>3</sub>	Trichlorofluoromethane	21.437	2.00	0.322	0.4641
C <sub>1</sub> H <sub>2</sub> Cl <sub>2</sub>	Dichloromethane	16.438	1.414	1.829	0.3635
C <sub>1</sub> H <sub>2</sub> ClBr	Bromochloromethane	19.255	1.414	1.704	0.04067
C <sub>1</sub> H <sub>3</sub> Cl	Chloromethane	11.312	1.00	2.113	0.02747
C <sub>1</sub> H <sub>3</sub> F	Fluoromethane	6.569	1.00	1.932	0.02021
C <sub>1</sub> HCl <sub>3</sub>	Trichloromethane	21.364	1.732	1.203	0.0447
C <sub>1</sub> HF <sub>2</sub> Cl	Chlorodifluoromethane	11.695	1.732	1.518	0.03087
C <sub>1</sub> HFCI <sub>2</sub>	Dichlorofluoromethane	16.529	1.732	1.377	0.03791
C <sub>2</sub> H <sub>6</sub>	Ethane	11.004	1.00	0.00	0.03089
C <sub>2</sub> H <sub>6</sub> O	Dimethyl Ether	13.012	1.414	1.394	0.03527
C <sub>2</sub> H <sub>6</sub> S	Ethanethiol	19.136	1.414	1.775	0.04598
C <sub>2</sub> H <sub>6</sub> S	Dimethyl sulfide	19.187	1.414	1.742	0.045
C <sub>3</sub> H <sub>6</sub> Cl <sub>2</sub>	1,2-dichloropropane	25.074	2.27	1.964	0.06001
C <sub>3</sub> H <sub>8</sub>	Propane	15.605	1.414	0.077	0.04211
C <sub>3</sub> H <sub>8</sub> S	1-propanethiol	23.66	1.914	1.758	0.05808
C <sub>3</sub> H <sub>8</sub> S	2-propanethiol	23.555	1.732	1.849	0.0576
C <sub>3</sub> H <sub>8</sub> S	Ethyl methyl sulfide	23.935	1.914	1.706	0.058
C <sub>4</sub> H <sub>10</sub>	Butane	20.206	1.914	0.00	0.05413
C <sub>4</sub> H <sub>10</sub>	2-methyl propane	20.154	1.732	0.118	0.05423
C <sub>4</sub> H <sub>10</sub> O	Diethyl ether	22.509	2.414	1.31	0.05892
C <sub>4</sub> H <sub>10</sub> S	1-methyl-1-propanethiol	28.079	2.27	1.822	0.06892
C <sub>4</sub> H <sub>10</sub> S	2-methyl-1-propanethiol	28.132	2.27	1.678	0.0695
C <sub>4</sub> H <sub>10</sub> S	2-methyl-2-propanethiol	28.192	2.00	1.834	0.06972
C <sub>4</sub> H <sub>10</sub> S	Diethyl sulfide	28.683	2.414	1.656	0.06946
C <sub>4</sub> H <sub>9</sub> Cl	1-chlorobutane	25.185	2.414	2.262	0.06317
C <sub>5</sub> H <sub>11</sub> Cl	1-chloro-2-methylpropane	29.657	2.808	2.31	0.07468
C <sub>5</sub> H <sub>12</sub>	Pentane	24.807	2.414	0.07	0.06582
C <sub>5</sub> H <sub>12</sub> S	tert-Butyl methyl sulfide	32.991	2.561	1.712	0.08139
C <sub>6</sub> H <sub>12</sub>	Cyclohexane	27.606	3.00	0.00	0.0717

$C_6H_{14}$	Hexane	29.408	2.914	0.00	0.07767
$C_7H_{16}$	Heptane	34.009	3.414	0.00	0.09004
$F_6S$	Sulfur hexafluoride	9.008	2.449	0.00	0.03761

Table 4  
Individual Surface Plotting Results

Type of surface	A (m <sup>2</sup> /g)	No. data points	Parameters	r <sup>2</sup> value
Carbopack C	10	27	MR	0.9163
			$\chi$	0.6613
			$\mu$	0.0007
			MR + $\chi$	0.9196
			MR + $\chi$ + $\mu$	0.9198
Carbopack B	100	17	MR	0.9719
			$\chi$	0.6173
			$\mu$	0.2545
			MR + $\chi$	0.9754
			MR + $\chi$ + $\mu$	0.9796
Super Sorb	3169	7	MR	0.8293
			$\chi$	0.3860
			$\mu$	0.0002
			MR + $\chi$	0.8299
			MR + $\chi$ + $\mu$	0.9855

Table 5

In  $B_{2s}$  vs. In Surface Area

<b>Molecule</b>	<b><math>r^2</math> value</b>
Propane	1
Dichloromethane	0.9996
Chloromethane	0.9992
Chlorodifluoromethane	0.9985

Table 6

 $r^2$  values for all In  $B_{2s}$  data

<b>Parameters</b>	<b><math>r^2</math></b>
MR	0.0855
MR, $\chi$ , $\mu$ , In A, $\ln(Vm^{1/3}/MR^{1/2})$	0.9623
MR, In A	0.9534
$\chi$ , In A	0.7759
$\mu$ , In A	0.4307
MR, $\chi$ , In A	0.9562
MR, $\chi$ , $\mu$ , In A	0.9566

## Table of Symbols

$B_{2s}$	second-gas virial coefficient
MR	molar refractivity
$\chi$	connectivity index
$\mu$	dipole moment
N	Avogadro's number
$\alpha$	polarizability
$\Sigma$	summation
$\delta$	# adjacent bonded nonhydrogen atoms
s	a bond in a molecule
t	corrected retention time
$F_1$	corrected flow rate of gas chromatographic column
m	mass of solid adsorbent
$t_m$	retention time of marker gas
$t_s$	retention time of sample gas
A	surface area of adsorbent
$z^*$	equilibrium internuclear gas-solid separation
$u_{1s}$	gas-solid interaction potential
y	reduced variable
k	Boltzmann constant
T	Temperature (Kelvin)
z	gas-solid separation

$nm$	Lennard-Jones exponential attractive/repulsive term
$E^*$	gas-solid interaction energy (Kelvin)
$B$	slope from linear plot of $E^*$ versus $MR$
$i$	intercept from linear plot of $E^*$ versus $MR$
$V_m$	molar volume
$V$	volume
$r$	radius

**Figure 1**  
**Predicting  $\ln B_{2s}$  on Carbopack C: MR**  $y = 0.9759x - 0.0182$   
 $R^2 = 0.9182$

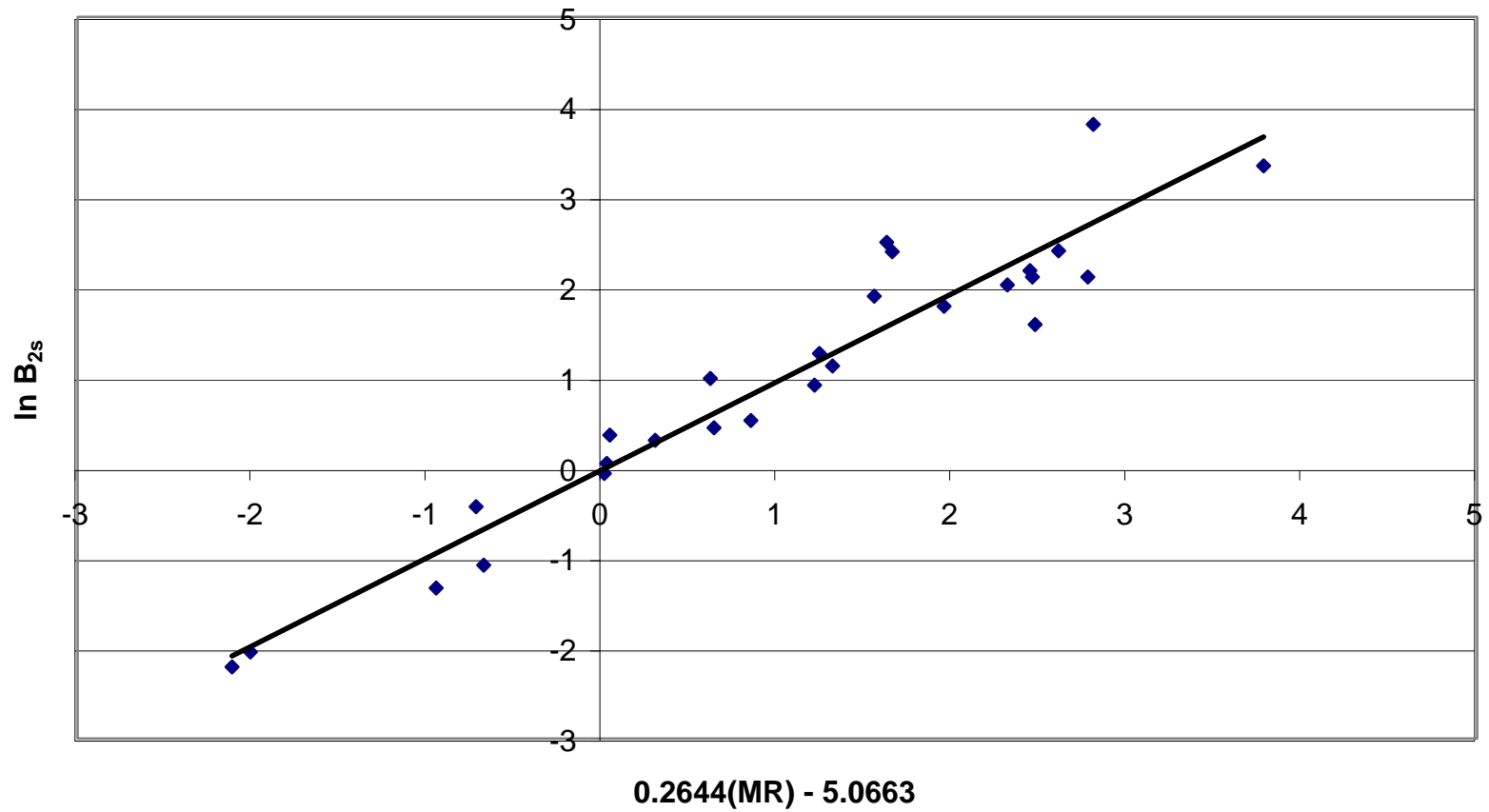
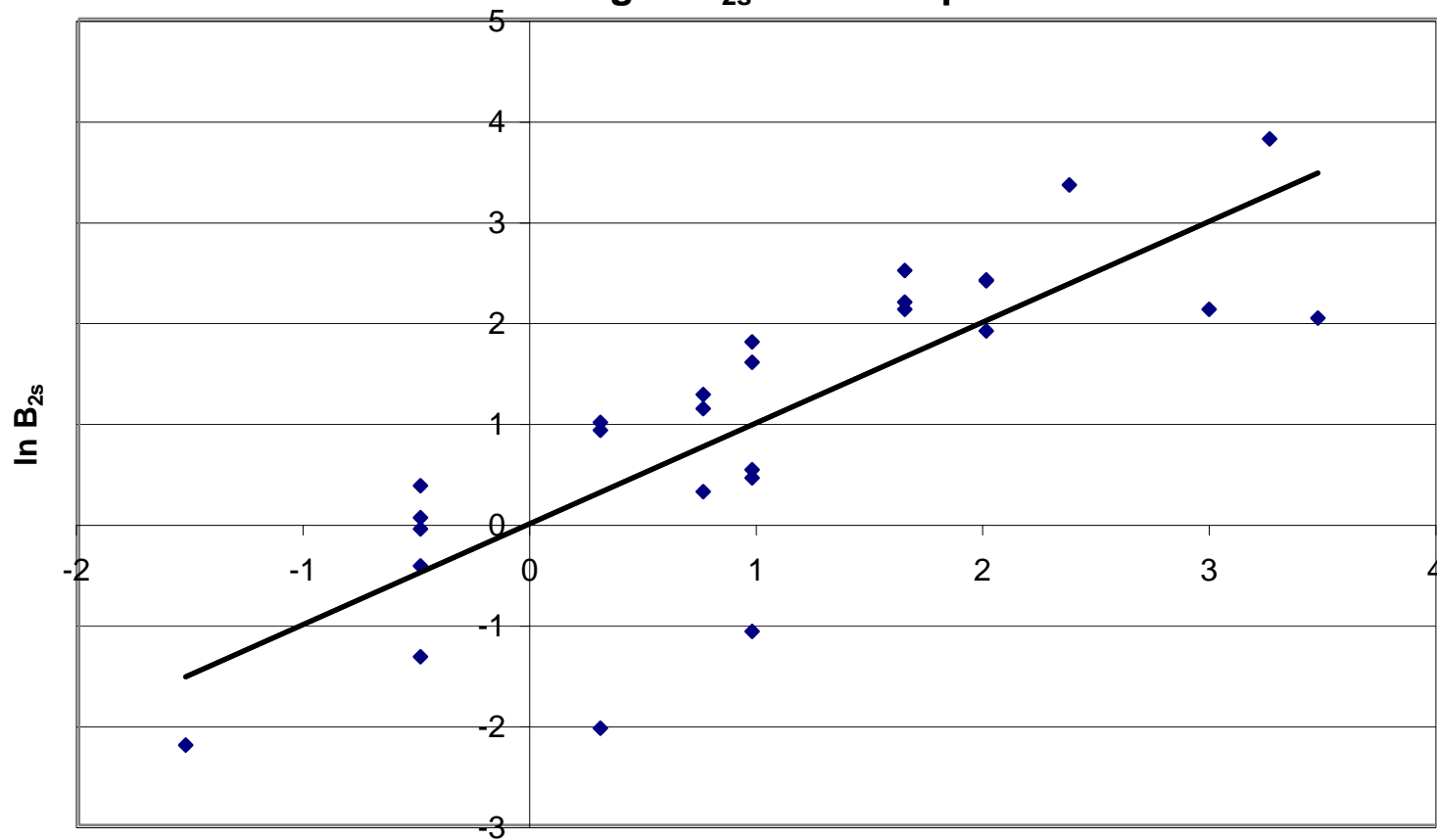


**Figure 2**  
**Predicting  $\ln B_{2s}$  on Carbopack C: C**

$y = 0.9999x + 0.0001$   
 $R^2 = 0.6612$



$2.4983 (c) - 4.0270$

**Figure 3**  
**Predicting  $\ln B_{2s}$  on Carbopack C: m**  $y = 0.9758x + 0.0242$   
 $R^2 = 0.0007$

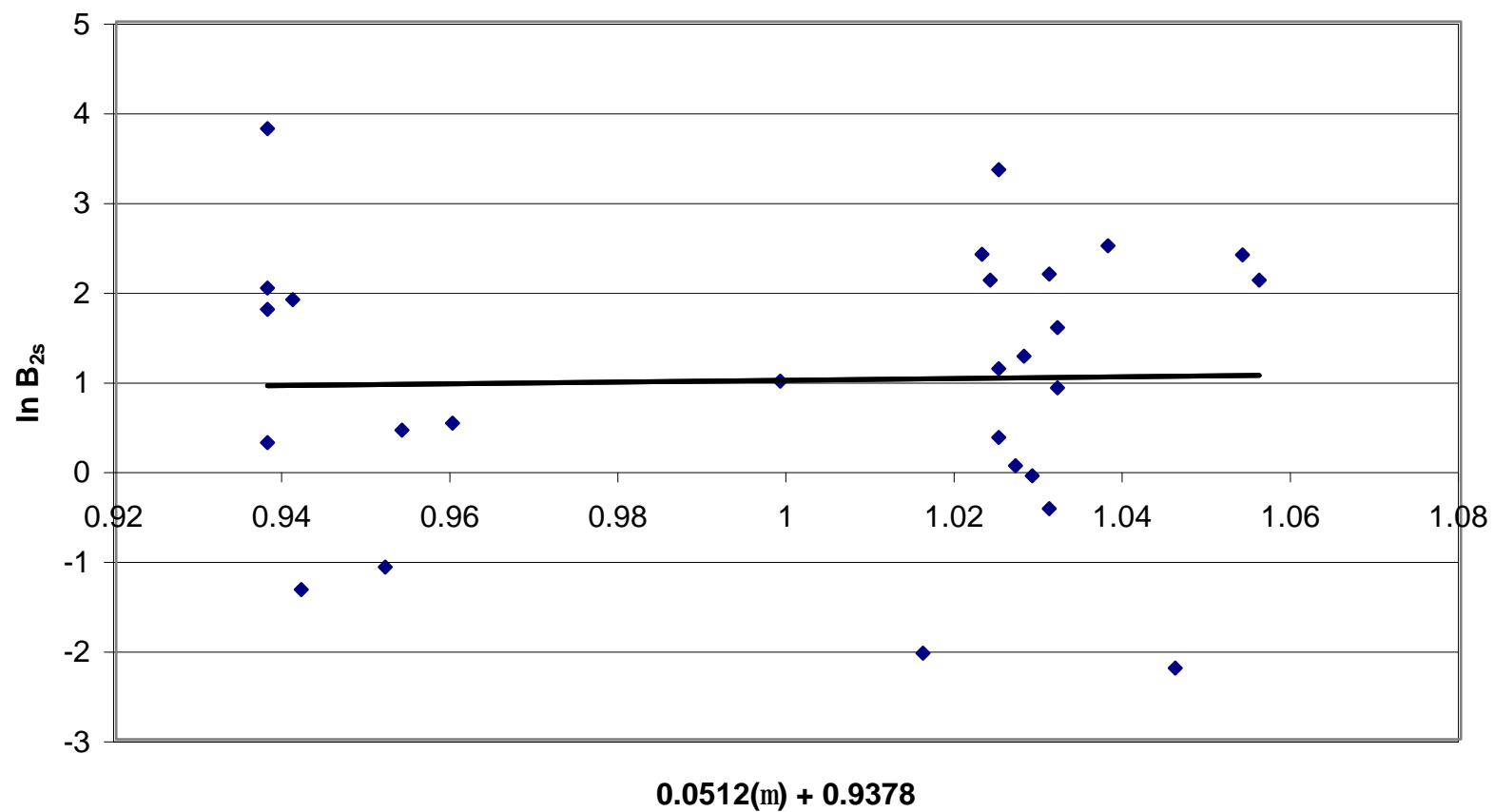


**Figure 4**  
**Predicting  $\ln B_{2s}$  on Carbopack C: MR + c**

$$y = x - 5E-06$$
$$R^2 = 0.9196$$

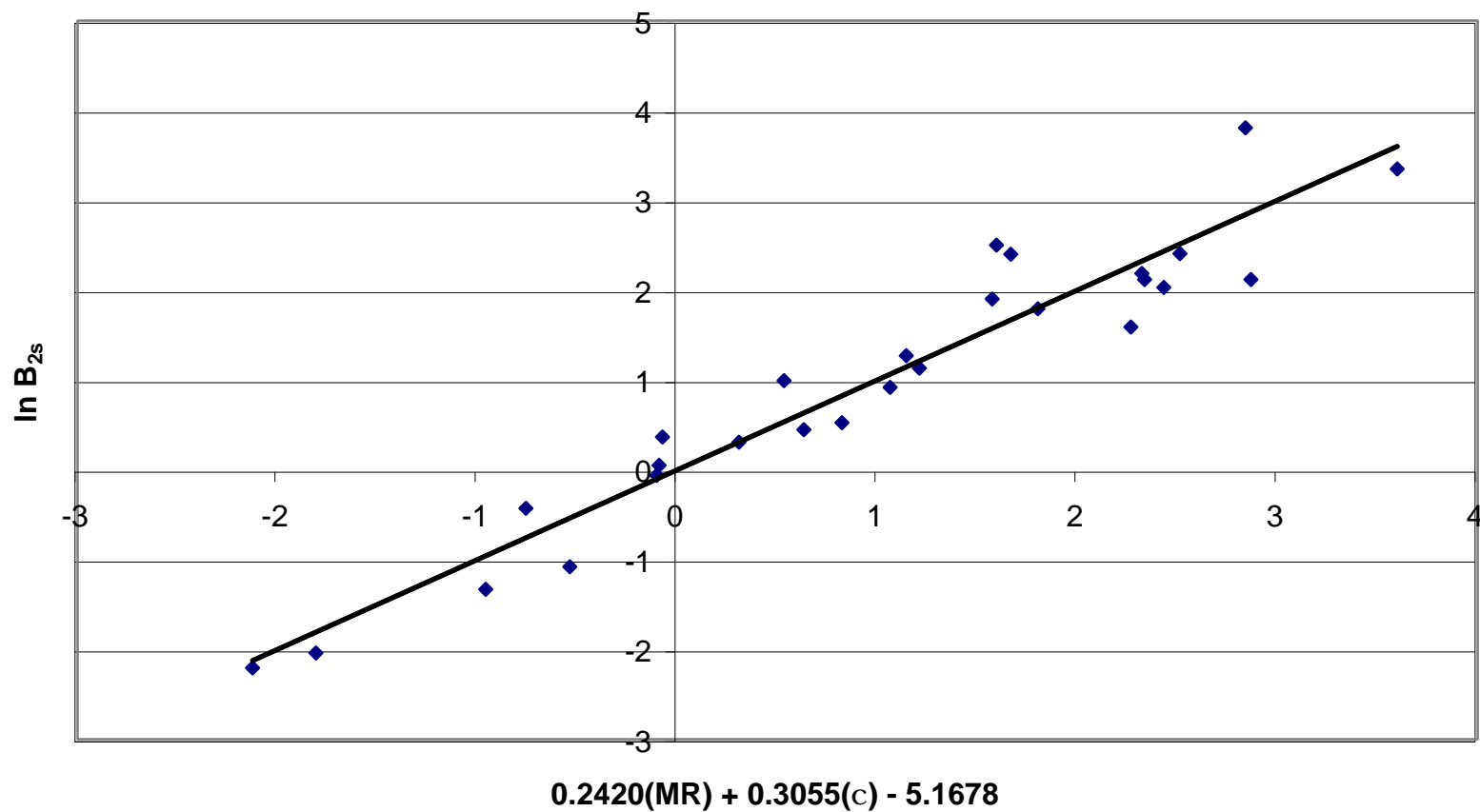
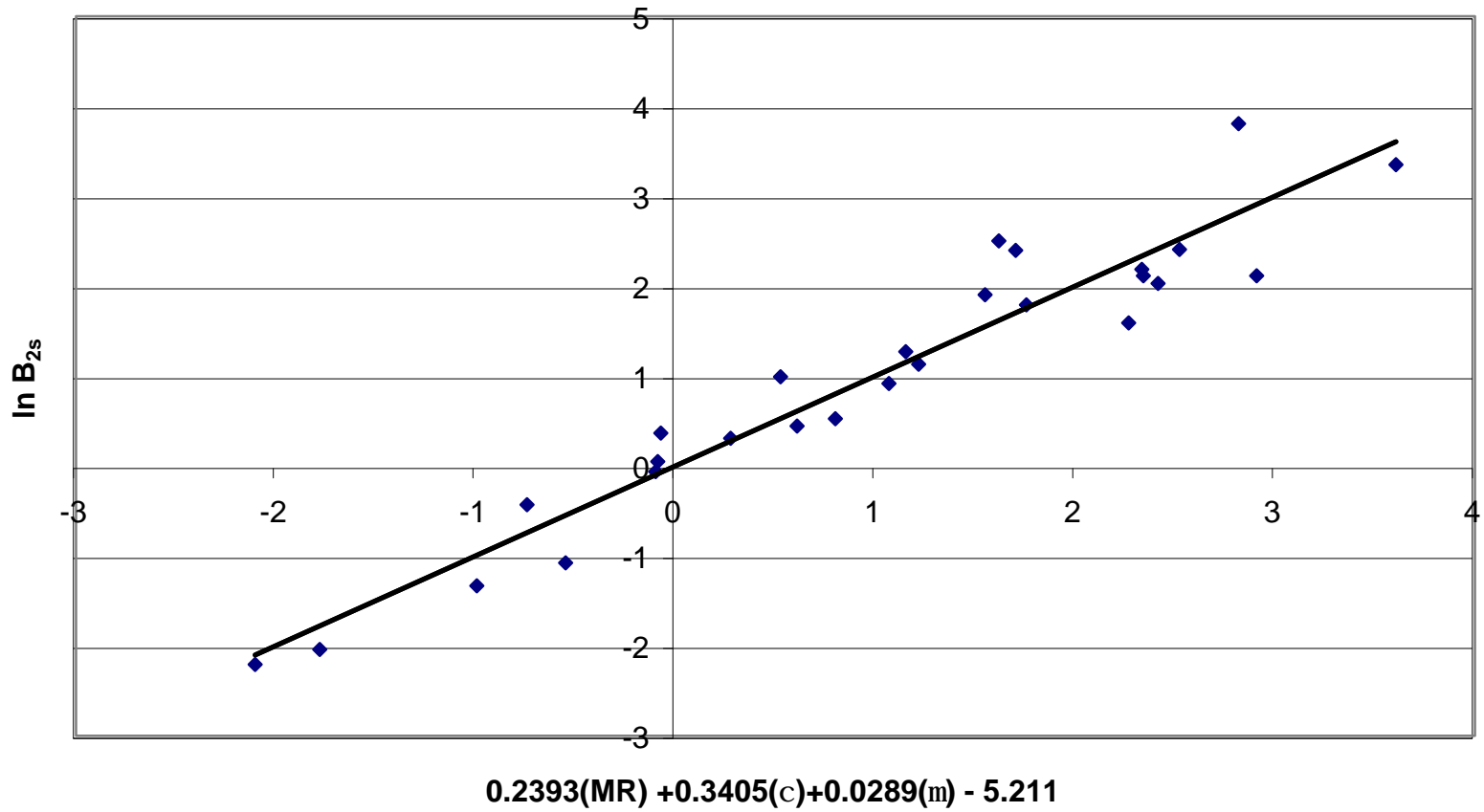


Figure 5

Predicting  $B_{2s}$  on Carbopack C: MR+ c+ m  $y = 0.9999x + 0.0001$   
 $R^2 = 0.9198$



**Figure 6**  
**Predicting  $\ln B_{2s}$ : MR**

$y = 1.0004x - 0.001$   
 $R^2 = 0.0855$

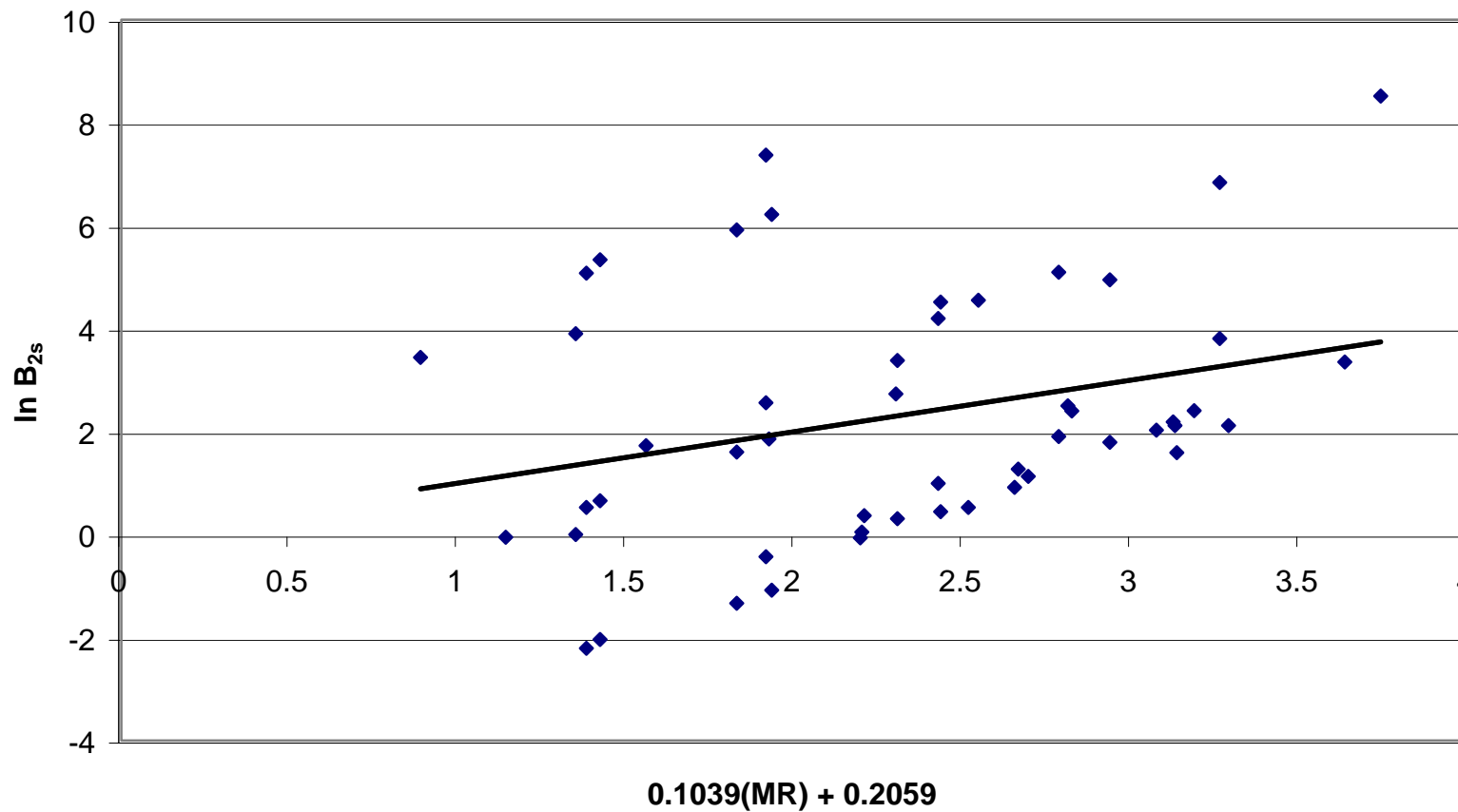
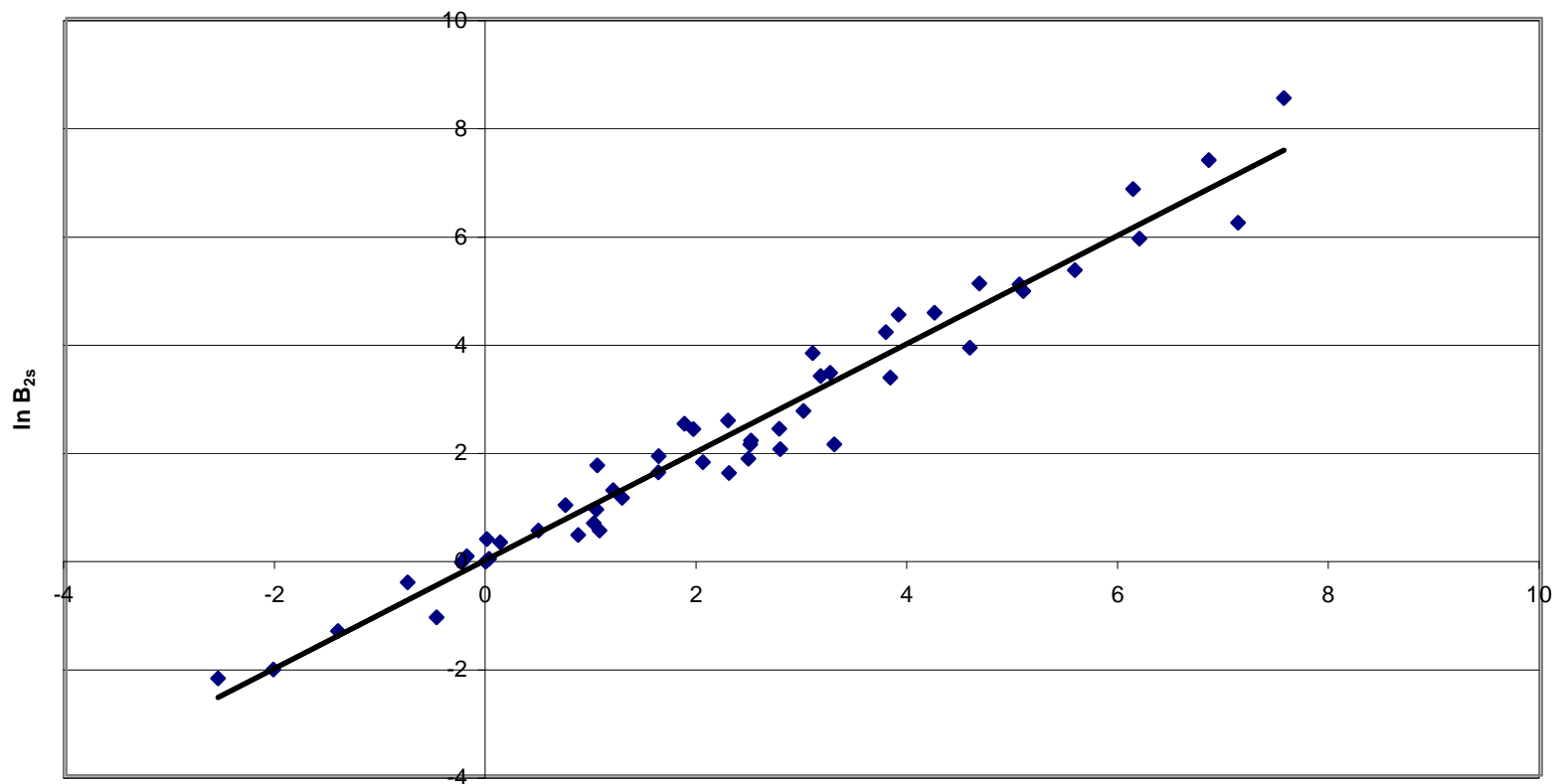


Figure 7

Predicting  $\ln B_{2s}$ :  $MR + c + m + \ln A + \ln(Vm^{1/3} / MR^{1/2})$

$$y = x + 2E-05$$

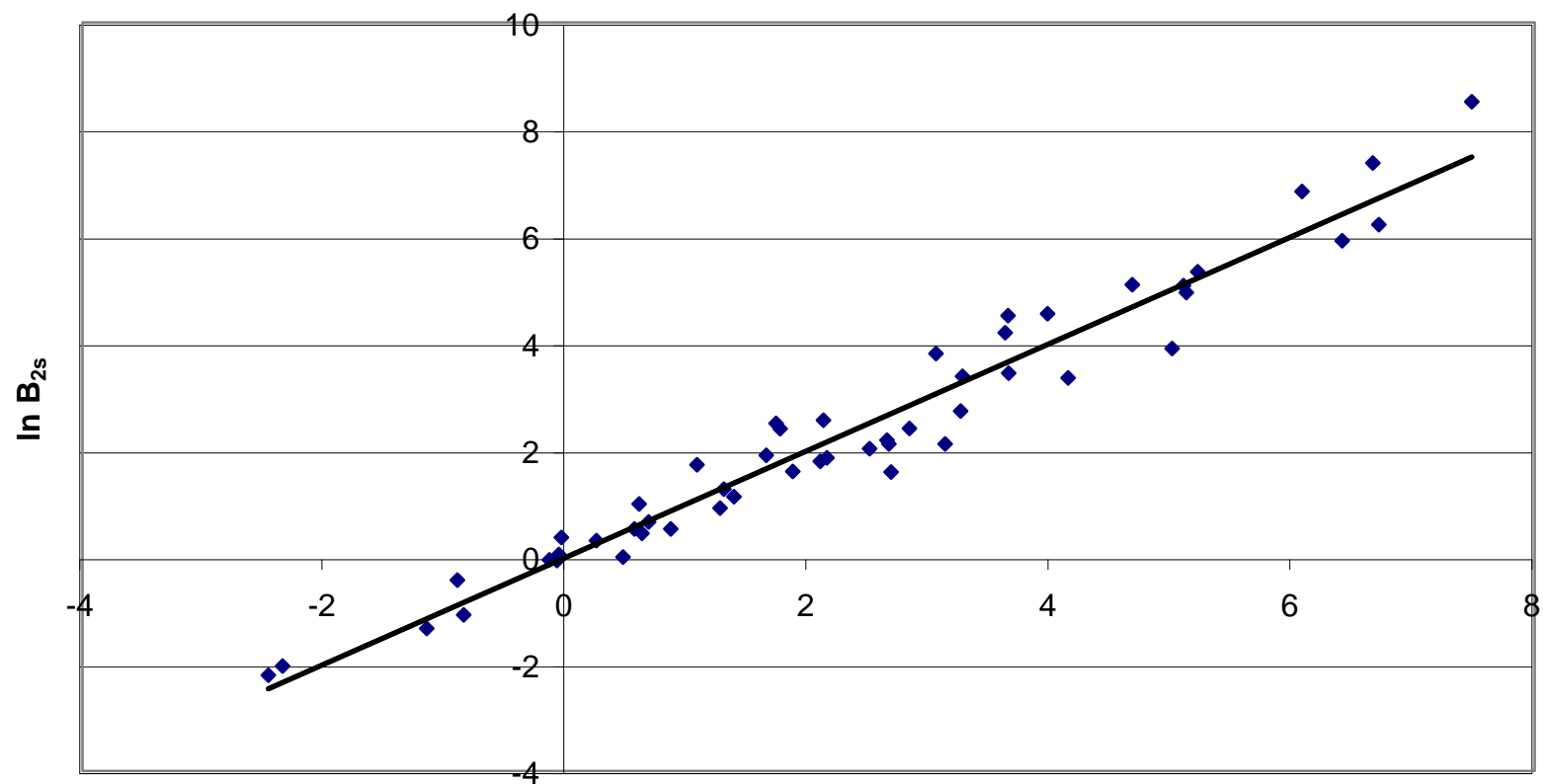
$$R^2 = 0.9623$$



$$0.1959(MR) + 0.8237(c) + 0.0675(m) + 1.3204(\ln A) - 5.038(\ln(Vm^{1/2}/MR^{1/2})) - 20.930$$

**Figure 8**  
**Predicting  $\ln B_{2s}$ : MR +  $\ln A$**

$$y = x - 1E-05$$
$$R^2 = 0.9534$$



$$\ln B_{2s} = 0.3049(\ln A) + 1.3134$$

**Figure 9**  
**Predicting  $\ln B_{2s}$ :  $C + \ln A$**

$$y = x + 0.0001$$
$$R^2 = 0.7759$$

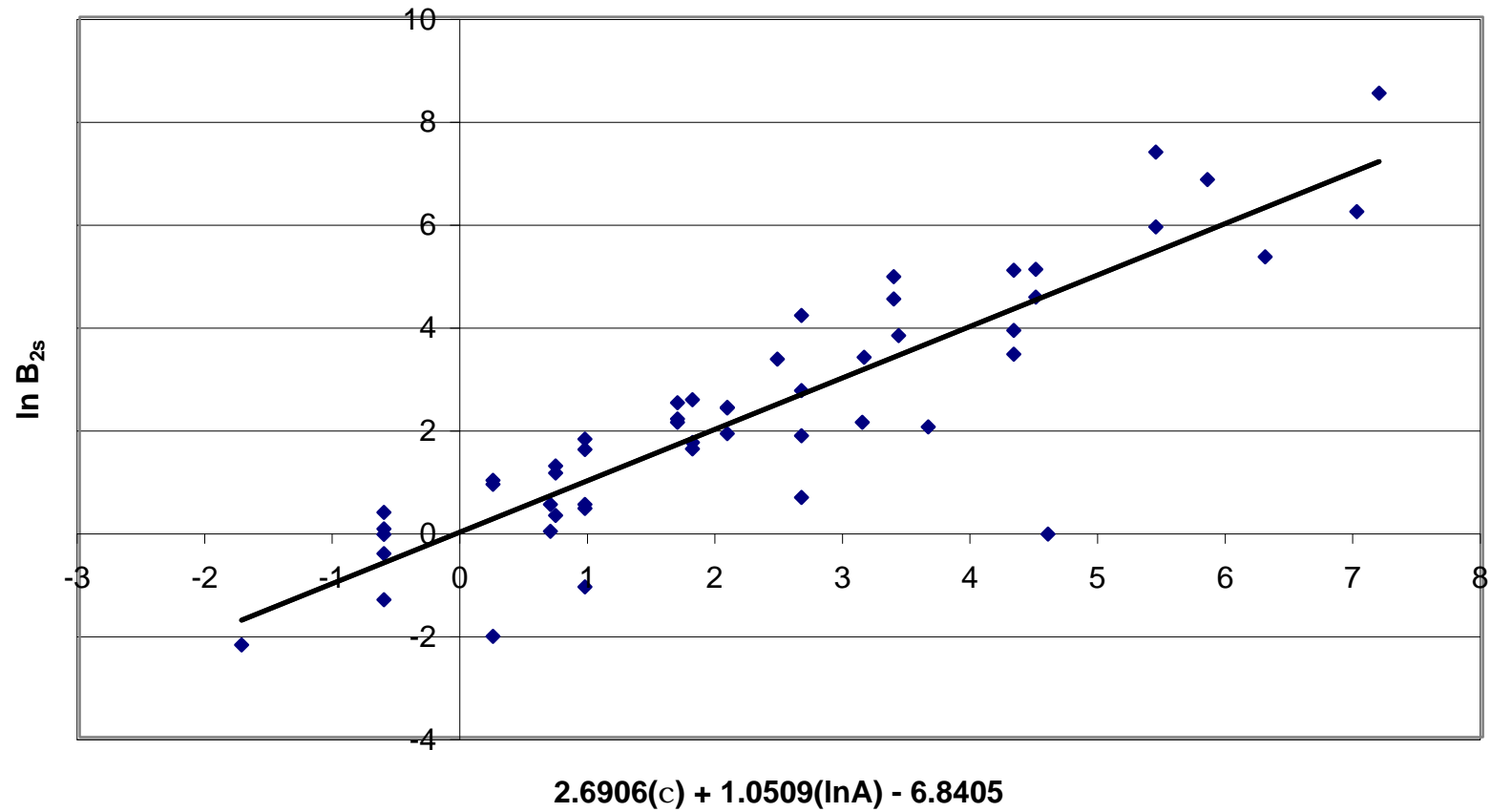


**Figure 10**  
**Predicting  $\ln B_{2s}$ :  $m + \ln A$**

$$y = x - 2E-05$$
$$R^2 = 0.4307$$

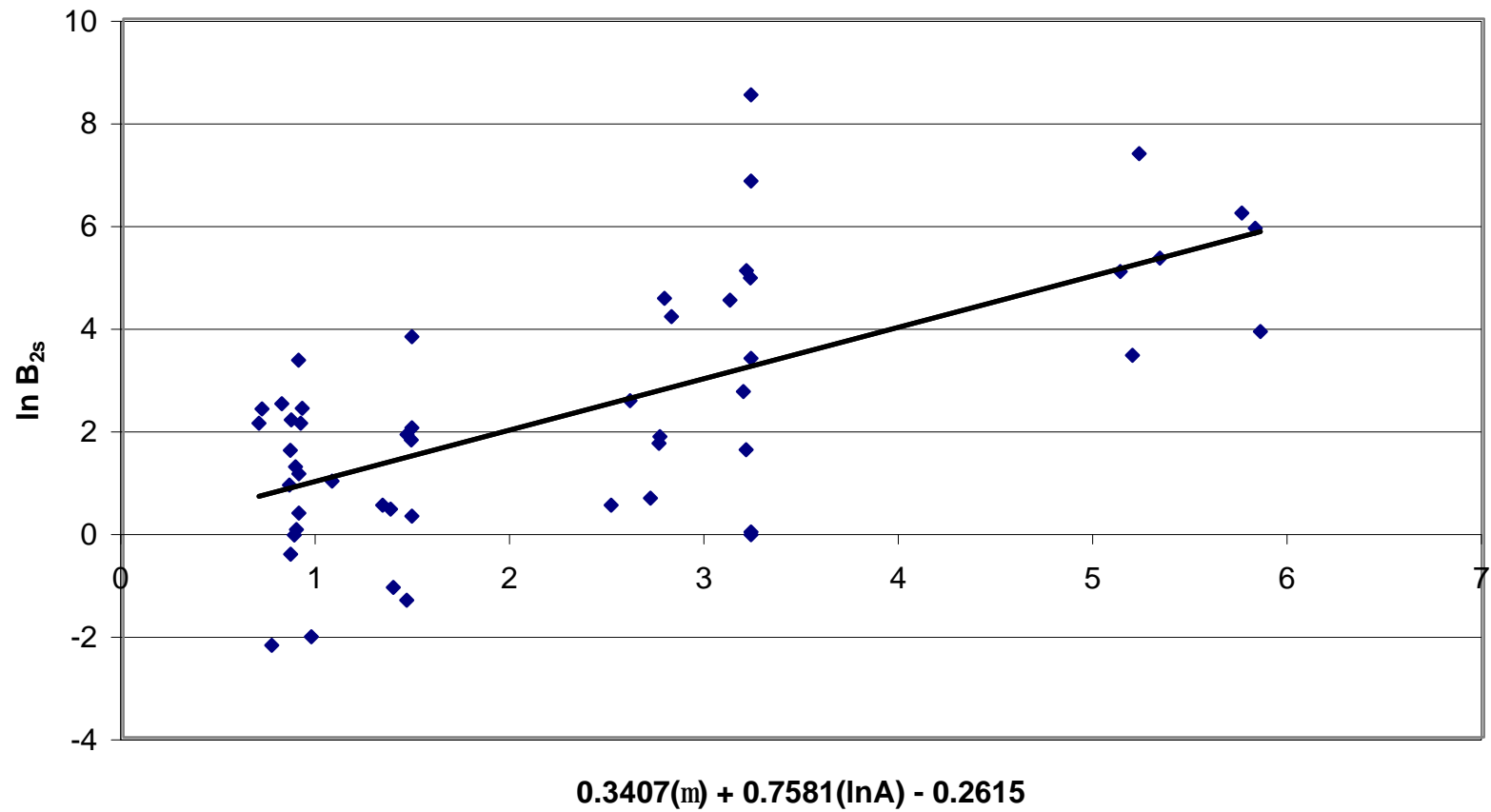


**Figure 11**  
**Predicting  $\ln B_{2s}$ : MR + c + lnA**

$y = x - 4E-05$   
 $R^2 = 0.9562$

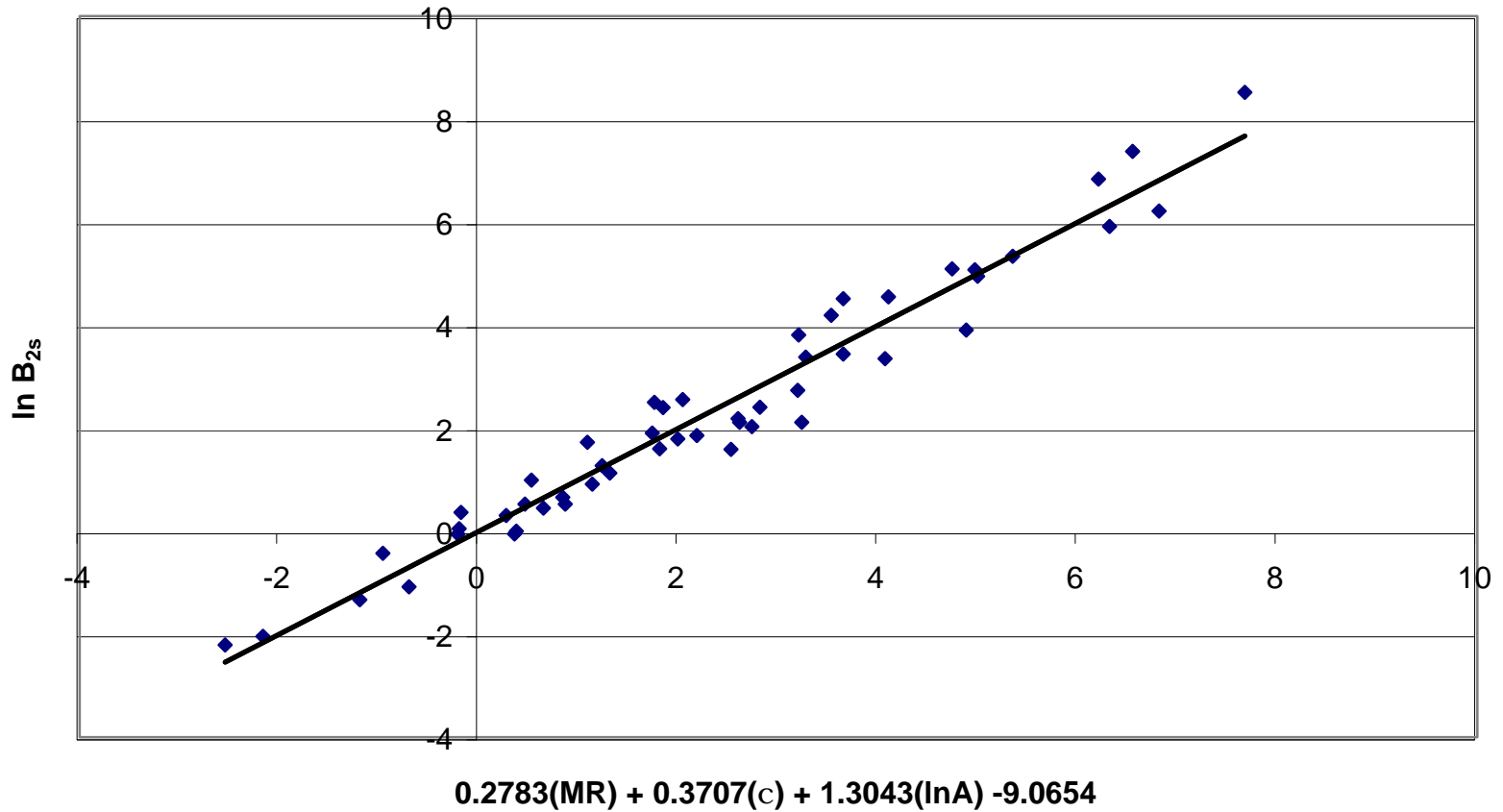


**Figure 12**  
**Predicting  $\ln B_{2s}$ : MR + c + m +  $\ln A$**

$$y = x + 3E-05$$
$$R^2 = 0.9566$$

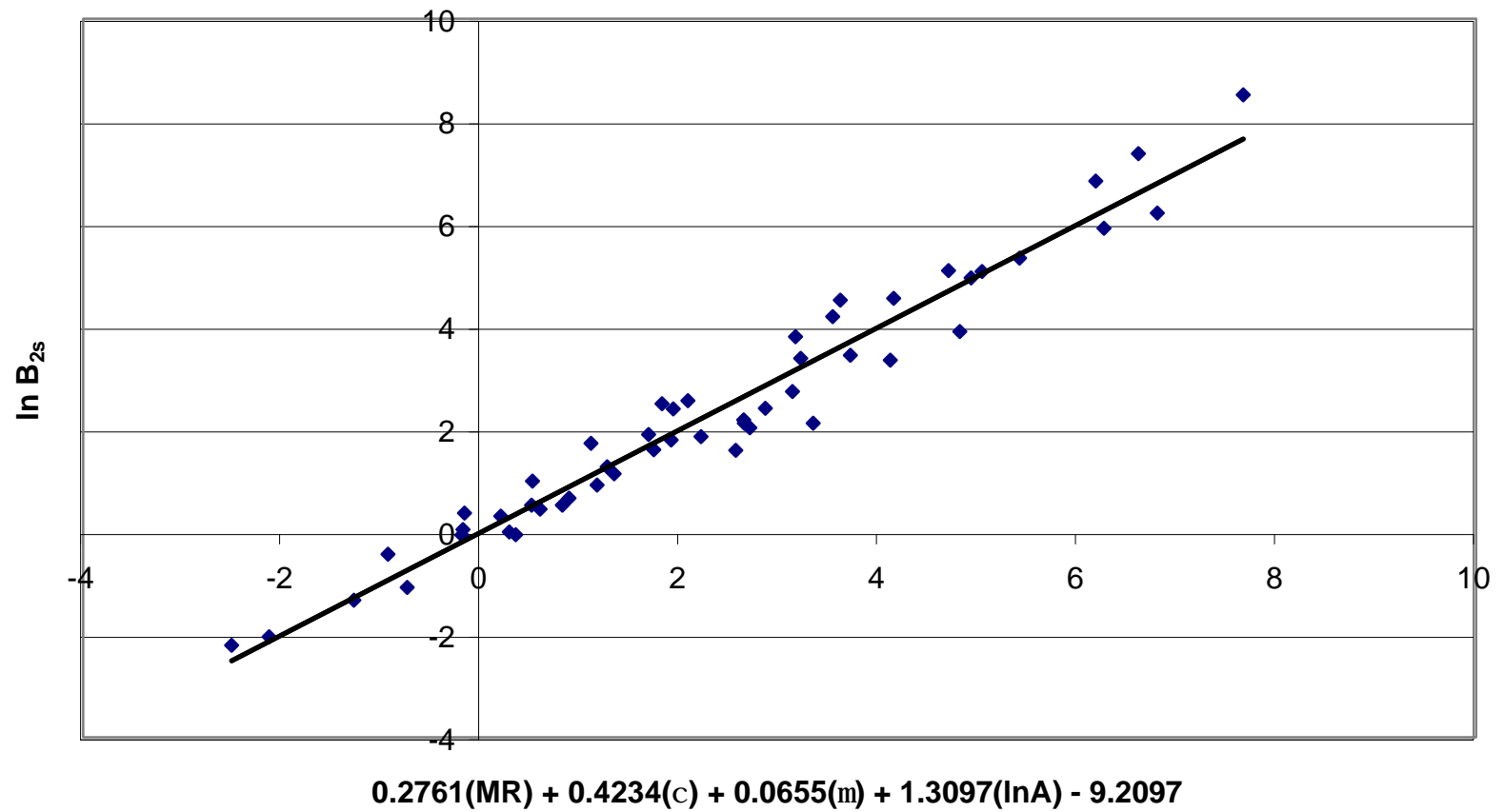


## Table of Symbols

$B_{2s}$	second-gas virial coefficient
MR	molar refractivity
$\chi$	connectivity index
$\mu$	dipole moment
N	Avogadro's number
$\alpha$	polarizability
$\Sigma$	summation
$\delta$	# adjacent bonded nonhydrogen atoms
s	a bond in a molecule
t	corrected retention time
$F_1$	corrected flow rate of gas chromatographic column
m	mass of solid adsorbent
$t_m$	retention time of marker gas
$t_s$	retention time of sample gas
A	surface area of adsorbent
$z^*$	equilibrium internuclear gas-solid separation
$u_{1s}$	gas-solid interaction potential
y	reduced variable
k	Boltzmann constant
T	Temperature (Kelvin)
z	gas-solid separation

MR	ln B2s	CI	ln B2s	MR,CI	ln B2s	DM	ln B2s	MR.Ci,DM	ln B2s
0.011	-0.062	-0.494	-0.062	-0.105	-0.062	1.029	-0.062	-0.1	-0.062
0.024	0.049	-0.494	0.049	-0.092	0.049	1.027	0.049	-0.089	0.049
1.626	2.501	1.644	2.501	1.594	2.501	1.038	2.501	1.618	2.501
-0.95	-1.332	-0.494	-1.332	-0.959	-1.332	0.942	-1.332	-0.994	-1.332
1.241	1.27	0.755	1.27	1.143	1.27	1.028	1.27	1.152	1.27
1.212	0.916	0.3	0.916	1.062	0.916	1.032	0.916	1.068	0.916
1.316	1.131	0.755	1.131	1.209	1.131	1.025	1.131	1.217	1.131
0.302	0.307	0.755	0.307	0.307	0.307	0.938	0.307	0.275	0.307
2.443	2.186	1.644	2.186	2.321	2.186	1.031	2.186	2.333	2.186
2.458	2.116	1.644	2.116	2.334	2.116	1.024	2.116	2.341	2.116
2.474	1.589	0.97	1.589	2.266	1.589	1.032	1.589	2.268	1.589
2.607	2.407	2.004	2.407	2.511	2.407	1.023	2.407	2.521	2.407
2.774	2.116	2.988	2.116	2.867	2.116	1.056	2.116	2.908	2.116
1.656	2.398	2.004	2.398	1.665	2.398	1.054	2.398	1.702	2.398
1.553	1.902	2.004	1.902	1.573	1.902	0.941	1.902	1.548	1.902
3.779	3.35	2.37	3.35	3.598	3.35	1.025	3.35	3.604	3.35
2.314	2.028	3.468	2.028	2.43	2.028	0.938	2.028	2.415	2.028
2.805	3.807	3.254	3.807	2.839	3.807	0.938	3.807	2.817	3.807
0.849	0.525	0.97	0.525	0.821	0.525	0.96	0.525	0.799	0.525
-0.678	-1.079	0.97	-1.079	-0.539	-1.079	0.952	-1.079	-0.55	-1.079
0.637	0.445	0.97	0.445	0.631	0.445	0.954	0.445	0.608	0.445
1.952	1.792	0.97	1.792	1.801	1.792	0.938	1.792	1.756	1.792
0.043	0.365	-0.494	0.365	-0.076	0.365	1.025	0.365	-0.074	0.365
-0.723	-0.431	-0.494	-0.431	-0.758	-0.431	1.031	-0.431	-0.744	-0.431
-2.117	-2.207	-1.529	-2.207	-2.125	-2.207	1.046	-2.207	-2.103	-2.207
0.617	0.993	0.3	0.993	0.532	0.993	0.999	0.993	0.525	0.993
-2.013	-2.04	0.3	-2.04	-1.808	-2.04	1.016	-2.04	-1.78	-2.04

MR + ln SA	CI + ln SA	ln B2s	DM + ln SA	ln B2s	MR, CI, ln SA	ln B2s	MR, CI, DM, ln B2s	MR	ln B2s	
0.466	0.69	0	3.229	0	0.374	0	0.284	0	1.35	0
5.005	4.322	3.904	5.849	3.904	4.882	3.904	4.81	3.904	1.35	3.904
1.079	1.804	1.728	2.755	1.728	1.087	1.728	1.105	1.728	1.559	1.728
-0.079	-0.616	-0.062	0.879	-0.062	-0.212	-0.062	-0.195	-0.062	2.195	-0.062
-0.063	-0.616	0.049	0.89	0.049	-0.198	0.049	-0.183	0.049	2.2	0.049
1.732	1.687	2.501	0.815	2.501	1.757	2.501	1.819	2.501	2.812	2.501
-1.155	-0.616	-1.332	1.458	-1.332	-1.195	-1.332	-1.281	-1.332	1.828	-1.332
1.869	1.804	1.601	3.203	1.601	1.808	1.601	1.734	1.601	1.828	1.601
6.408	5.436	5.919	5.823	5.919	6.316	5.919	6.261	5.919	1.828	5.919
1.301	0.73	1.27	0.885	1.27	1.232	1.27	1.265	1.27	2.665	1.27
1.268	0.24	0.916	0.854	0.916	1.135	0.916	1.165	0.916	2.654	0.916
1.384	0.73	1.131	0.903	1.131	1.309	1.131	1.337	1.131	2.694	1.131
0.248	0.73	0.307	1.484	0.307	0.271	0.307	0.196	0.307	2.306	0.307
3.272	3.15	3.381	3.229	3.381	3.274	3.381	3.212	3.381	2.306	3.381
3.256	2.659	2.734	3.189	2.734	3.192	2.734	3.128	2.734	2.301	2.734
3.974	4.495	4.551	2.783	4.551	4.1	4.551	4.145	4.551	2.546	4.551
2.648	1.687	2.186	0.863	2.186	2.594	2.186	2.64	2.186	3.125	2.186
2.664	1.687	2.116	0.912	2.116	2.609	2.116	2.645	2.116	3.13	2.116
2.682	0.96	1.589	0.859	1.589	2.525	1.589	2.558	1.589	3.136	1.589
2.832	2.075	2.407	0.92	2.407	2.815	2.407	2.857	2.407	3.187	2.407
3.129	3.135	2.116	0.697	2.116	3.232	2.116	3.336	2.116	3.289	2.116
1.766	2.075	2.398	0.713	2.398	1.842	2.398	1.931	2.398	2.824	2.398
1.65	2.075	1.902	1.46	1.902	1.737	1.902	1.683	1.902	2.785	1.902
4.674	4.495	5.094	3.206	5.094	4.74	5.094	4.698	5.094	2.785	5.094
4.145	2.469	3.35	0.901	3.35	4.068	3.35	4.112	3.35	3.635	3.35
2.504	3.651	2.028	1.484	2.028	2.733	2.028	2.699	2.028	3.075	2.028
3.053	3.42	3.807	1.484	3.807	3.202	3.807	3.16	3.807	3.263	3.807
6.077	5.84	6.836	3.229	6.836	6.206	6.836	6.176	6.836	3.263	6.836
7.48	7.185	8.518	3.229	8.518	7.672	8.518	7.658	8.518	3.741	8.518
0.861	0.96	0.525	1.334	0.525	0.863	0.525	0.817	0.525	2.516	0.525
-0.851	0.96	-1.079	1.388	-1.079	-0.7	-1.079	-0.744	-1.079	1.932	-1.079
6.712	7.012	6.215	5.754	6.215	6.811	6.215	6.797	6.215	1.932	6.215
0.623	0.96	0.445	1.374	0.445	0.645	0.445	0.593	0.445	2.434	0.445
3.647	3.38	4.516	3.12	4.516	3.649	4.516	3.609	4.516	2.434	4.516
2.097	0.96	1.792	1.481	1.792	1.991	1.792	1.908	1.792	2.937	1.792
5.121	3.38	4.949	3.226	4.949	4.994	4.949	4.924	4.949	2.937	4.949

-0.042	-0.616	0.365	0.903	0.365	-0.179	0.365	-0.167	0.365	2.207	0.365
-0.901	-0.616	-0.431	0.861	-0.431	-0.963	-0.431	-0.936	-0.431	1.915	-0.431
2.123	1.804	2.557	2.606	2.557	2.04	2.557	2.079	2.557	1.915	2.557
6.662	5.436	7.371	5.226	7.371	6.548	7.371	6.605	7.371	1.915	7.371
-2.464	-1.73	-2.207	0.764	-2.207	-2.543	-2.207	-2.509	-2.207	1.382	-2.207
0.56	0.69	0.525	2.51	0.525	0.46	0.525	0.507	0.525	1.382	0.525
5.099	4.322	5.075	5.129	5.075	4.968	5.075	5.033	5.075	1.382	5.075
3.653	4.322	3.44	5.191	3.44	3.648	3.44	3.712	3.44	0.889	3.44
2.151	2.659	1.855	2.76	1.855	2.183	1.855	2.209	1.855	1.924	1.855
0.601	0.24	0.993	1.074	0.993	0.526	0.993	0.517	0.993	2.427	0.993
3.625	2.659	4.194	2.82	4.194	3.529	4.194	3.533	4.194	2.427	4.194
-2.347	0.24	-2.04	0.967	-2.04	-2.165	-2.04	-2.132	-2.04	1.422	-2.04
0.677	2.659	0.658	2.712	0.658	0.838	0.658	0.884	0.658	1.422	0.658
5.216	6.292	5.338	5.332	5.338	5.346	5.338	5.41	5.338	1.422	5.338
-0.142	4.59	-0.051	3.229	-0.051	0.356	-0.051	0.346	-0.051	1.142	-0.051